ACS APPLIED MATERIALS & INTERFACES

Research Article

www.acsami.org

Fabrication of a Self-Cleaning Surface via the Thermosensitive Copolymer Brush of P(NIPAAm-PEGMA)

Yuansong Ye,[†] Jian Huang,*[,†] and Xiaolin Wang[‡]

[†]College of Material Science and Engineering, Nanjing Tech University, Nanjing 210009, China

[‡]Department of Chemical Engineering, Tsinghua University, Beijing 100084, China

Supporting Information

ABSTRACT: Surface hydrophilicity and the inherent washing force are two crucial factors for constructing an underwater self-cleaning surface. Following this self-cleaning mechanism, we fabricated thermosensitive copolymer brushes of *N*-isopropylacrylamide (NIPAAm) and poly(ethylene glycol) methacrylate (PEGMA) on the polypropylene (PP) surface. Benefiting from the hydrophilic poly(ethylene glycol) (PEG) side chains, the copolymer brushes with the PEGMA content exceeding 5 mol % exhibited good surface hydrophilicity, whenever at temperatures below or above the lower critical solution temperatures (LCST). Hence their underwater oleophobicity was greatly improved with oil contact angles higher than 141° and oil adhesive forces lower than 20 μN. In addition, the sharp volume-phase transition feature was reserved in their copolymer backbones, as proved by the AFM result. Self-cleaning evaluation of the modified surfaces was performed by a simple temperature-change water cleaning method, after which only 0.2 wt % of oil residues remained on the brush surface of P(NIPAAm-5PEGMA) (with 5 mol % of PEGMA contents). The excellent self-cleaning capability is believed to be ascribed to its balanced surface features in hydrophilicity and the sharper volume-phase transition, when a hydrophilic surface can facilitate oil desorption and an intense conformation change of chain stretching and shrinking can offer the strong washing force to assist oil detachment. This study contributes to development of the underwater self-cleaning surface based on a hydrophilic surface with the chain motion.

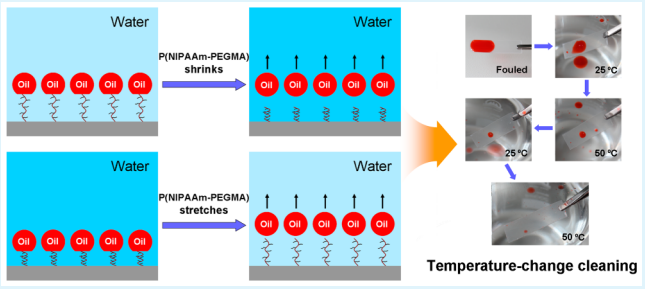

KEYWORDS: *self-cleaning surface, poly(N-isopropylacrylamide), poly(ethylene glycol), surface hydrophilicity, volume-phase transition, washing force*

1. INTRODUCTION

Self-cleaning surfaces for prevention or removal of oil fouling have attracted extensive attention due to their potential applications in industry, agriculture, and daily life.[1−4] Many outstanding self-cleaning surfaces with oil contact angles higher than 150° have been fabricated by constructing the hierarchical micro/nanostructure of fluorinated materials on the solid surface.[2−4] However, limited by their low surface energy, these self-cleaning surfaces are only available in an air environment due to easy adhesion to oil pollutants in an aqueous medium.[5] Recently, inspired by the excellent underwater-oil-repellent capability of natural shark skins or carp scales,[6,7] various hydrophilic materials are employed for preparing superoleophobic surfaces, such as polymer brushes,[8,9] hydrogels,[10,11] as well as inorganic oxides.[12,13] These hydrophilic materials extend the self-cleaning application to the aqueous environment and are promising to be used in many practical areas, including membrane separation,[9] marine antifouling coating,[12] oil/water separation,[8,11,13] and microfluidic technology.[10]

A hydrophilic surface is known to be easily hydrated upon immersed in water so that a low interface tension is produced between solid/water (γ_{sw}).[14] Therefore, a similar interface tension of solid/oil (γ_{so}) to that of oil/water (γ_{ow}) can be induced. On the basis of these interface features, the hydrophilic surface tends to present underwater oleophobicity with the high oil contact angle (θ), as indicated by the Young equation (eq 1):[13]

$$-\cos\theta = \frac{\gamma_{so} - \gamma_{sw}}{\gamma_{ow}} \quad (1)$$

To some extent, this oleophobicity of the hydrophilic surface is similar to that of a solid surface immersed in an aqueous solution with surfactants, when both interfacial tensions of γ_{sw} and γ_{ow} are significantly decreased due to surfactant adsorption.[15] According to the washing principle, an oil pollutant is spontaneously detachable from the solid surface if its contact angle reaches 180°.[16,17] However, it is seldom that an oil pollutant can reach such a high contact angle limited by the surfactant ability in lowering the interfacial tensions of γ_{sw} and γ_{ow}.[17] Therefore, the additional mechanical force is usually

Received: February 14, 2015
Accepted: September 21, 2015
Published: September 21, 2015

DOI: 10.1021/acsami.5b07336
ACS Appl. Mater. Interfaces 2015, 7, 22128−22136

required for assisting the thorough detachment of pollutants from the surface (see the Supporting Information, Figure S1), such as the hydrodynamic flow action or abrasion action of the fabric used in traditional washing.[18,19] For most hydrophilic surfaces, it is still difficult to display such underwater superoleophobicity because of their insufficient surface hydrophilicity.[10,12] Hence, the natural shark and carp utilize the hydrodynamic flow action via swimming to resist oil fouling. For the artificial hydrophilic surface, however, it is a challenge to provide the washing force for achieving the thorough removal of oil pollutants.

Poly(*N*-isopropylacrylamide) (PNIPAAm) is a well-known thermoresponsive polymer that exhibits the volume-phase transition at the lower critical solution temperature (LCST) of 32 °C.[20,21] A rapid conformation change of chain stretching and shrinking always occurs accompanying its hydrophilicity−hydrophobicity change in the volume-phase transition. For this reason, more than 10 times the volume change[22] and 8 times the surface stress change[23] can be induced for PNIPAAm when its chains in the shrinking state are turned into the stretching state. These unique characters of PNIPAAm can endow its surface with the self-cleaning performance.[24−27] For example, Huang[24] proved that the PNIPAAm graft chain on the microporous membrane surface accelerated pollutant detachment. After a simple temperature-change water cleaning around the LCST, the fouled membrane finally reached a flux recovery of 97.6%. Similarly, Zhou[25] also reported a high flux recovery of about 80% for the PNIPAAm-grafted microporous ZrO_2 membrane fouled by bovine serum albumin (BSA). The temperature-change cleaning method was still valid by simply diffusing free PNIPAAm into the pollutant layer. As a result, the fouled polyamide reverse osmosis membrane achieved a flux recovery of 89.3%.[26] These self-cleaning performances are apparently attributed to good hydrophilicity of PNIPAAm below the LCST and the strong conformation change in the volume-phase transition. The reason is that the hydrophilic surface can facilitate pollutant desorption and the conformation change of chain stretching and shrinking can provide the strong washing force to accelerate pollutant detachment. Nevertheless, the surface hydrophobicity of PNIPAAm at temperatures above the LCST is unfavorable for the pollutant desorption due to its easy adhesion property to pollutants.[28,29] Small amounts of pollutants inclined to remain on the surface after the temperature-change cleaning cycles.[24,25] Therefore, the surface hydrophobicity of PNIPAAm is an evident defect for fabricating a promising self-cleaning surface utilizing its unique volume-phase transition feature.

On the basis of various valuable characters of water-solubility and biocompatibility, poly(ethylene glycol) (PEG) is one of the most frequently studied and used polymers in polymer modification.[30−32] For example, the PEG side chain in a copolymer can effectively prevent the polymer backbone from interaction with plasma proteins and cells, and is therefore used as the shielding agent for in vivo delivery of several bioactive compounds.[33,34] For thermosensitive PNIPAAm, incorporating small amounts of the comonomer can mainly reserve its volume-phase transition feature except shifting its LCST to slightly higher temperatures or lower temperatures.[35,36] Therefore, Kwon[37] could create a thermosensitive surface with a rapid hydration rate via introducing PEG side chains into PNIPAAm. Utilizing hydrophilic PEG and thermoresponsive PNIPAAm, Husson[38−40] has prepared antifouling and self-cleaning membranes for treatment of produced water by grafting PNIPAAm-*block*-poly((polyethylene glycol) methacrylate) (P(PEGMA)) on the membrane surface. The PNIPAAm-*block*-P(PEGMA) grafted membrane exhibited antifouling and self-cleaning performances similar to those by the PNIPAAm grafted membrane.[39] The reason is maybe that the P(PEGMA) block in PNIPAAm-*block*-P(PEGMA) is imperfect due to the low reinitiation efficiency of PNIPAAm in the atom transfer radical polymerization (ATRP)[38] or that the bare PNIPAAm block cannot effectively resist oil fouling in its hydrophobic state. In this work, we prepared thermoresponsive copolymer brushes of NIPAAm and PEGMA by the simple random copolymerization way. The PEG side chain in the random copolymers can keep stretched in an aqueous solution benefiting from its hydrophilicity, whenever at temperatures below or above LCSTs of the copolymers. Hence the PEG side chains around the copolymer backbone could greatly improve surface hydrophilicity of PNIPAAm via the shielding effect at temperatures above the LCST. Thus, a self-cleaning surface with less pollutant adsorption can be created on the basis of the unique volume-phase transition feature of PNIPAAm.

2. EXPERIMENTAL SECTION

2.1. Materials. *N*-Isopropylacrylamide (NIPAAm) was purchased from Kasei Kogyo Co., Ltd. (Tokyo, Japan) and recrystallized in hexane for purification. Poly(ethylene glycol) methacrylate (PEGMA) (M_n = 300) was received from Internet Aladdin Reagent Database Inc. (Shanghai, China) and used without further purification. Polypropylene (PP) film with size of 3.5 cm × 1 cm and thickness of 200 μm was cleaned with acetone prior to use. Hexadecane (98.0%) was sourced from Sinopharm Chemical Reagent Co., Ltd. (Shanghai, China) and used as received.

2.2. Preparation of Copolymer Brushes. The plasma apparatus used for surface treatment of PP films was homemade, as described in our previous work.[41] After the plasma treatment in an argon atmosphere of 30 Pa, under the plasma power of 7 W for 3 min, the PP film was exposed in air to produce peroxide groups on the surface. Graft polymerization from the peroxide groups was carried out in the monomer aqueous solution (7 wt % of NIPAAm and PEGMA, 8.0×10^{-5} mol/L of the Mohr's salt) at 50 °C for 5 h. Both monomers of NIPAAm and PEGMA were in molar ratios of 100/0, 98/2, 95/5, 91/9, 87/13, and 0/100, and their polymer brushes were referred to as PNIPAAm, P(NIPAAm-2PEGMA), P(NIPAAm-5PEGMA), P(NIPAAm-9PEGMA), P(NIPAAm-13PEGMA), and P(PEGMA), respectively. The grafted films were immersed in water overnight to remove nonreacted monomers and free polymers.

2.3. Characterizations. *2.3.1. FT-IR Analysis.* Surface chemistries of modified surfaces were analyzed using a NEXUS 670 spectrometer (Nicolet) equipped with an attenuated total reflectance (ATR) accessory. Spectra were obtained with a total of 32 scans and a resolution of 4 cm^{-1}.

2.3.2. Contact Angle Measurement. Contact angles were recorded on a DSA 100 drop shape analysis system (Krüss, Germany) equipped with a temperature-control unit. Water contact angles were measured with a 2 μL water droplet at the temperature range from 25 to 55 °C. By syringing a 2 μL oil droplet (hexadecane) onto the modified surface underwater, oil contact angles were measured at both temperatures of 25 and 50 °C. Each contact angle value reported was an average of at least five independent measurements.

2.3.3. Transmittance Measurement. The lower critical solution temperatures (LCST) of thermosensitive polymer brushes were measured using an UV-2000 UV−visible spectrometer (Unico, China) at the wavelength of 500 nm, when free polymers formed in graft solutions were adopted. The polymer aqueous solution was preheated to 60 °C and then allowed it to cool to room temperature. Both changes of transmittance and the temperature were simultaneously recorded, from which the midpoint temperature of the sharp

DOI: 10.1021/acsami.5b07336
ACS Appl. Mater. Interfaces 2015, 7, 22128−22136

transmittance transition was referred to as the LCST of the thermosensitive polymer.

2.3.4. Adhesive Force Measurement. The adhesive force of modified surfaces was measured following the same principle of Liu,[7] using a BSA124S microelectronic balance (Sartorius, Germany). Typically, the sample was placed on the bottom of a container filled with water, which stayed on the weighing pan of the balance. An oil droplet (hexadecane, 2 μL) suspended in a metal O-ring was moved downward to contact the sample surface and then drawn away slowly from the surface at a given speed of 0.01 mm/s. The force change was continuously recorded by the balance software and the maximal force occurring when the oil droplet left the surface was referred to as the adhesive force of the modified surface. All adhesive force measurements were carried out at both temperatures of 25 and 50 °C, respectively. Each adhesive force value reported was an average of at least five independent measurements. During the adhesive force measurement, an optical microscope lens and a charge-coupled device (CCD) camera system were used to record the oil droplet shape.

2.3.5. AFM Observation. Hydrated samples of modified surfaces were frozen at −18 °C and then dried under vacuum, by which the thermosensitive brushes could keep stretched after water (ice) was evaporated. On the contrary, the heat-drying of the hydrated samples was performed at 60 °C, a temperature higher than all LCSTs of the thermosensitive brushes. Hence the thermosensitive brushes could keep shrunk on the dried surfaces. Surface morphologies of thermosensitive brushes were observed on a Dimension Edge atomic force microscope (AFM, Bruker). All images were obtained in the tapping mode at the room temperature by using a Si_3N_4 AFM tip with spring constants of 0.025 N/m. AFM data were analyzed by NanoScope Analysis software.

2.4. Self-Cleaning Evaluation. The self-cleaning evaluation of the thermosensitive surfaces was carried out with hexadecane as the model oil. After depositing a drop of oil on the dried sample surface, the fouled sample was immersed in water without additional shaking for temperature-change cleaning. The temperature-change cleaning was performed alternately at 25 and 50 °C, lasting 2 min at each temperature. After the temperature-change cleaning cycle, the sample was taken out and dried under vacuum at the room temperature. Oil residues on the surface were weighed and calculated following the eq 2:

$$\text{oil residue} = \frac{W_2 - W_1}{W_0} \times 100\% \quad (2)$$

where W_1, W_2, and W_0 represent weights of the original sample, the fouled sample after the temperature-change cleaning, and the oil droplet of hexadecane, respectively. The temperature-change cleaning was repeated for three cycles following the same procedure mentioned above.

3. RESULTS AND DISCUSSION

3.1. Preparation of Copolymer Brushes. Copolymer brushes of P(NIPAAm-PEGMA) were grafted on the PP surface from peroxide groups induced by the argon plasma. Surface chemistries of the modified surfaces were analyzed by FT-IR and their spectra are shown in Figure 1a. The PNIPAAm component in the copolymer brushes was identified by both the presence of amide I (C═O stretching vibration) at 1648 cm^{-1} and amide II (C−N stretching vibration and N−H bending vibration) at 1542 cm^{-1}.[25] The P(PEGMA) component was identified by bands at 1727 and 1107 cm^{-1}, both stretching vibrations of C═O and C−O−C for PEGMA, respectively.[42] The proportional growth in peak strengths of 1727 cm^{-1} (see the Supporting Information, Figure S2) and 1107 cm^{-1} with an increase of PEGMA amounts verified that serial P(NIPAAm-PEGMA) brushes with various PEGMA ratios had been fabricated on the PP surface. For the P(NIPAAm-PEGMA) copolymer brush equipped with PEG

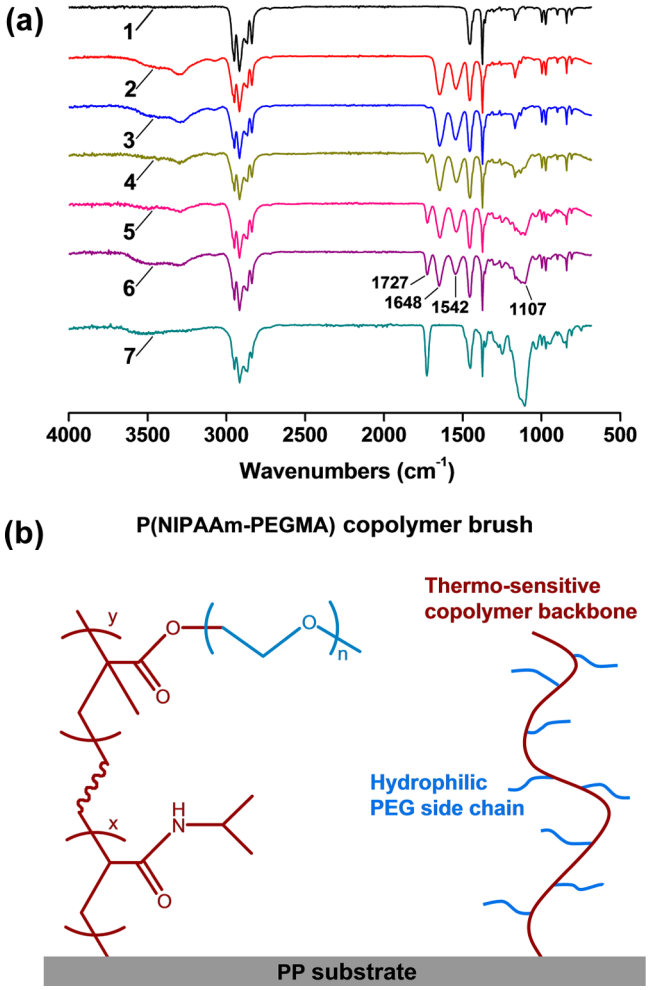

Figure 1. (a) FT-IR spectra of polymer brush surfaces: (1) original PP, (2) PNIPAAm, (3) P(NIPAAm-2PEGMA), (4) P(NIPAAm-5PEGMA), (5) P(NIPAAm-9PEGMA), (6) P(NIPAAm-13PEGMA), and (7) P(PEGMA). (b) Schematic illustration of the P(NIPAAm-PEGMA) copolymer brush grafted on the PP surface.

side chains, as sketched in Figure 1b, it is hoped that the copolymer backbone can reserve the volume-phase transition feature as that of PNIPAAm, simultaneously, the PEG side chains can improve surface hydrophilicity of the copolymer via their shielding effect.

3.2. Contact Angles. As a thermosensitive polymer, PNIPAAm is known to exhibit the sharp volume-phase transition at its LCST of about 32 °C in an aqueous solution.[20] The essential cause of the volume-phase transition is cleavage of hydrogen bonds between amide groups of PNIPAAm and bound water at temperatures above the LCST.[21] Therefore, a hydrophilicity−hydrophobicity transition of PNIPAAm always occurs in the volume-phase transition. For evaluating the hydrophilicity−hydrophobicity transition feature of P(NIPAAm-PEGMA) copolymers, both the water contact angle (in air) and oil contact angle (in water) were measured on their modified surfaces and their temperature dependences were discussed in detail.

As seen in water contact angle results of Figure 2a, all thermosensitive brushes showed significant contact angle transitions with temperature increase, from which midpoint temperatures were referred to as their LCSTs. The thermosensitive polymers showed enhanced LCST values

DOI: 10.1021/acsami.5b07336
ACS Appl. Mater. Interfaces 2015, 7, 22128−22136

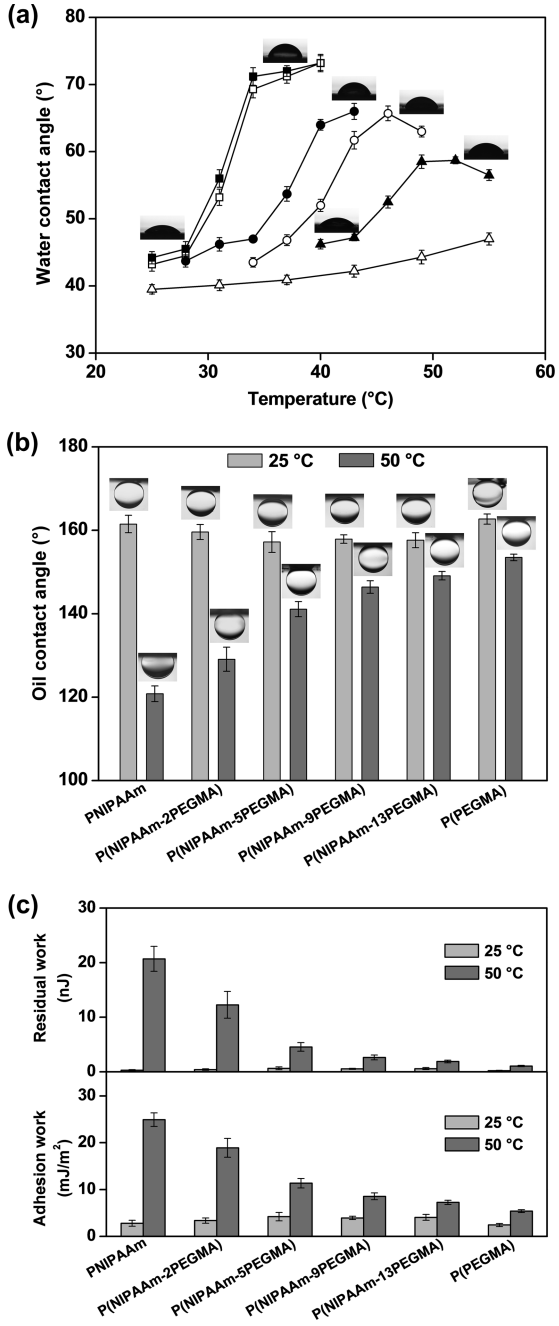

Figure 2. (a) Water contact angles on polymer brush surfaces as a function of the temperature: (■) PNIPAAm, (□) P(NIPAAm-2PEGMA), (●) P(NIPAAm-5PEGMA), (○) P(NIPAAm-9PEGMA), (▲) P(NIPAAm-13PEGMA), and (Δ) P(PEGMA). (b) Underwater-oil contact angles on polymer brush surfaces at temperatures of 25 and 50 °C, respectively. Insets in parts a and b show wetting behaviors of water or oil droplets on polymer brush surfaces under the corresponding conditions. (c) Adhesion works and residual works of oil droplets on polymer brush surfaces at temperatures of 25 and 50 °C, respectively.

from 31.5 °C of PNIPAAm to 31.7, 37.5, 40.7, and 46.2 °C for P(NIPAAm-2PEGMA), P(NIPAAm-5PEGMA), P(NIPAAm-9PEGMA), and P(NIPAAm-13PEGMA), respectively. This LCST enhancement is attributed to hydrogen bond strengthening between polymer segments and ambient water due to incorporation of hydrophilic PEGMA.[35] The LCSTs of the thermosensitive polymers were also measured by a transmittance method when their free polymers formed in graft solutions were adopted (see the Supporting Information, Figure S3). In result, both measuring methods exhibited similar LCST values for the thermosensitive polymers, except that the transmittance method showed sharper LCST transitions.[43] Interestedly, the P(NIPAAm-PEGMA) copolymers presented a linear growth of LCST values with increase of the PEGMA content (see the Supporting Information, Figure S3).

These contact angle changes well confirm reservation of the hydrophilicity−hydrophobicity transition in P(NIPAAm-PEGMA) copolymers after introducing the PEGMA comonomer, when lower contact angles were exhibited below their LSCTs and higher contact angles were shown above their LCSTs. Nevertheless, the P(NIPAAm-PEGMA) copolymers exhibited gradually decreased contact angles in the hydrophobic state with increase of the PEGMA content. In the end, the P(NIPAAm-PEGMA) copolymer brushes presented hydrophilic surfaces with contact angles below 66° at temperatures above the LCSTs when the PEGMA content exceeded 5 mol %. These hydrophilicity improvements are evidently beneficial from incorporation of the PEGMA comonomer, when the hydrophilic PEG side chain can effectively shield the hydrophobic polymer backbone.

Oil contact angles of the copolymer brush surfaces were also measured for evaluating their underwater oleophobicity, as results shown in Figure 2b. The measurement was performed with hexadecane as the model oil at both temperatures of 25 and 50 °C, between which all thermosensitive polymers located their LCSTs. As seen in Figure 2b, all thermosensitive brushes presented excellent surface superoleophobicity with oil contact angles higher than 150° in their hydrophilic states (25 °C). This superoleophobicity can be well interpreted by significant decrease in interface tensions of solid/water (γ_{sw}) of the hydrophilic surfaces, as indicated by the Young equation (eq 1). In contrast, the thermosensitive brushes exhibited inferior oleophobicity in their hydrophobic states (50 °C) due to the hydrophilicity−hydrophobicity transition. Nevertheless, the oleophobicity of the hydrophobic state presented a gradually enhanced tendency with an increase of the PEGMA content. Finally, both oil contact angles of 25 and 50 °C went closely for P(NIPAAm-PEGMA) copolymers with higher PEGMA contents. These oleophobicity improvements are attributed to hydrophilicity enhancement of the copolymer brushes at temperatures above LCSTs, as confirmed by their water contact angle results of Figure 2a.

On the basis of the above oil contact angle values (θ), both the adhesion work (W_a)[44] and the residual work (A_R)[45] of oil droplets on the surfaces (Figure 2c) can be calculated following eqs 3 and 4, respectively:

$$W_a = \gamma_{ow}(\cos\theta + 1) \tag{3}$$

$$A_R = \pi\left(\frac{3v}{\pi}\right)^{2/3}(\sqrt[3]{4} - \sqrt[3]{2 - 3\cos\theta + \cos\theta^3})\gamma_{ow} \tag{4}$$

Both calculations are on the basis of γ_{ow} values of 53.3 and 51.1 mJ/m^2 of hexadecane at 25 and 50 °C, respectively,[46] with the oil droplet volume (v) of 2 μL. According to the washing principle developed by Kling and his co-workers,[45,47] the A_R is the theoretical work required to drive the oil contact angle from its equilibrium value to 180°, aiming at complete oil detachment from the surface via the "rolling up" mechanism. Therefore, both W_a and A_R are good thermodynamic

DOI: 10.1021/acsami.5b07336
ACS Appl. Mater. Interfaces 2015, 7, 22128−22136

parameters for estimating oil detachability from the surface. That is to say, a low value of W_a or A_R means that the oil droplet prefers leaving the surface. As seen in Figure 2a and Figure 2c, all hydrophilic surfaces offered lower values of W_a and A_R than hydrophobic surfaces, suggesting an oil droplet is easily detachable from a hydrophilic surface. These thermodynamic results coincide exactly with above oil contact angle results in estimating the oil detachability.

3.3. Adhesive Forces. For further comprehending the oil detachability from the surfaces, oil adhesive forces were quantitatively measured using a microweight balance system. The adhesive force is the actual force needed to draw the oil droplet away from the surface. Hence, it is a much more direct parameter in evaluating oil detachability from a solid surface. Evidently, the adhesive force is closely related to underwater interaction of oil and solid at their interface, which depends on interface tensions of solid/oil (γ_{so}), oil/water (γ_{ow}), and solid/water (γ_{sw}). Because of thermal insensibility of the interface tension to the ambient temperature,[46] the adhesive force should be relatively stable to temperature change in a small range. Therefore, both fixed temperatures of 25 and 50 °C could be adopted in the adhesive force measurement to represent the hydrophilic and hydrophobic states of the thermosensitive brushes, respectively (see Figure 2a and Supporting Information Figure S3). The maximum values in the adhesive force curves were referred to as the adhesive forces of oil droplets, as results shown in Figure 3a and Supporting Information Figure S4. As expected, all hydrophilic surfaces (25 °C) presented lower adhesive force values of about 5 μN than hydrophobic surfaces (50 °C), giving similar results to those from W_a and A_R. P(NIPAAm-PEGMA) copolymers in the hydrophobic state exhibited a gradually declining tendency in adhesive forces with increase of the PEGMA content. In the end, both P(NIPAAm-9PEGMA) and P(NIPAAm-13PEGMA) gave almost the same adhesive force values as hydrophilic P(PEGMA), confirming the shielding effect of PEG side chains in inhibiting oil adhesion.

Figure 3b shows images of oil droplets before and after they left the surfaces, from which the oil detachability can also be evaluated. For all hydrophilic surfaces of thermosensitive brushes (25 °C) and the P(PEGMA) brush, the oil droplets maintained perfect sphericity at the moment they left the surfaces, and no oil residues remained on the surfaces. Nevertheless, the oil droplet exhibited seriously distorted sphericity on the hydrophobic surface of PNIPAAm (50 °C) and evident oil residues remained. This discrepancy reveals that an oil droplet would rather adhere to a hydrophobic surface than to a hydrophilic surface. Therefore, the oil droplet distortion and oil residues became alleviated on copolymer surfaces (50 °C) with higher PEGMA contents, benefiting from their hydrophilicity improvement. Both P(NIPAAm-9PEGMA) and P(NIPAAm-13PEGMA) only showed slightly distorted sphericity of oil droplets on the surfaces. Considering oil contact angle values of these thermosensitive surfaces, as shown in Figure 2b, it can be deduced that an oil droplet prefer not to adhere to a solid surface with an oil contact angle exceeding 145°.

3.4. Surface Morphologies. For thermosensitive PNIPAAm, a strong conformation change of chain stretching and shrinking always occurs accompanying its hydrophilicity–hydrophobicity change in the volume-phase transition. The conformation changes of thermosensitive brushes were observed by AFM on their modified surfaces after treatments

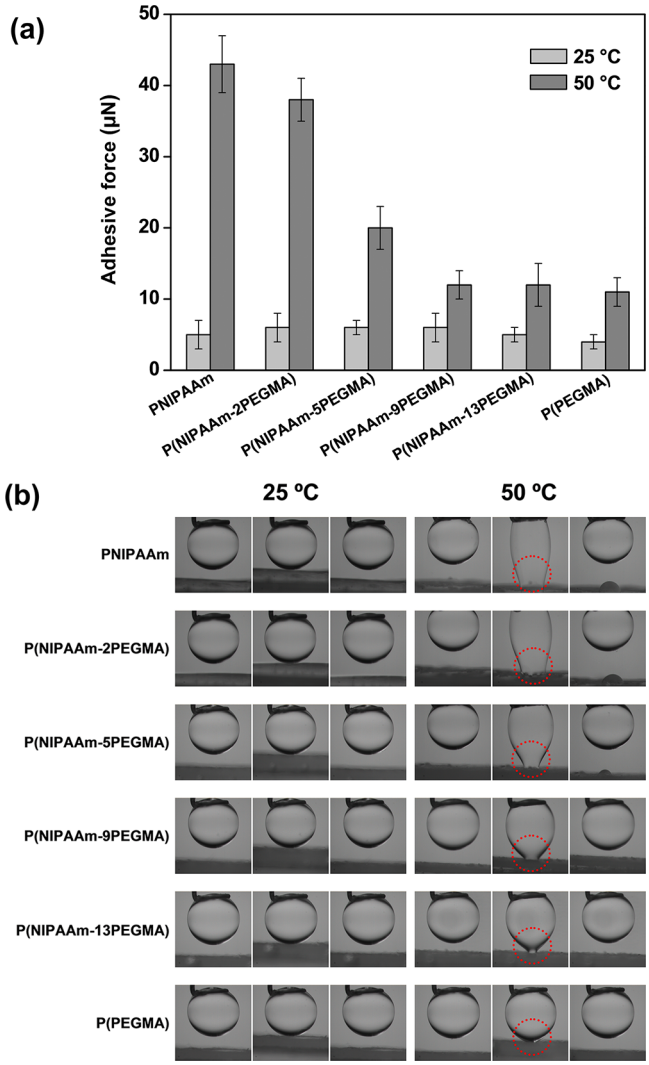

Figure 3. (a) Oil adhesive forces on polymer brush surfaces at temperatures of 25 and 50 °C. (b) Images of oil droplets before and after they were drawn away from polymer brush surfaces during the adhesive force measurement. For each samples at 25 or 50 °C, the left image represents the oil droplet before it contacted the surface, the middle image represents the oil droplet at the moment it left the surface, and the right image represents the oil droplet after it left the surface.

by freeze-drying and heat-drying, respectively. The freeze-drying method can allow the thermosensitive brushes to remain stretched after water (ice) was removed by vacuum, whereas the heat-drying method can allow them to keep shrunk on the surfaces. Hence this AFM measurement on both dried surfaces can really reflect the conformation change of chain stretching and shrinking of the thermosensitive brushes.

As seen in the AFM results of Figure 4, all thermosensitive brushes exhibited the significant morphologic discrepancy between the freeze-dried surface and heat-dried surface. They showed a "forest-shaped" morphology on the freeze-dried surface, representing the stretched chain in the hydrophilic state, and showed a "hill-shaped" morphology on the heat-dried surface, representing the shrunk chain in the hydrophobic state. In contrast, the P(PEGMA) homopolymer brush merely showed the "forest-shaped" morphology on both freeze-dried and heat-dried surfaces, indicating its insensitive character. Root-mean-square (RMS) roughness of the brush surfaces was

DOI: 10.1021/acsami.5b07336
ACS Appl. Mater. Interfaces 2015, 7, 22128–22136

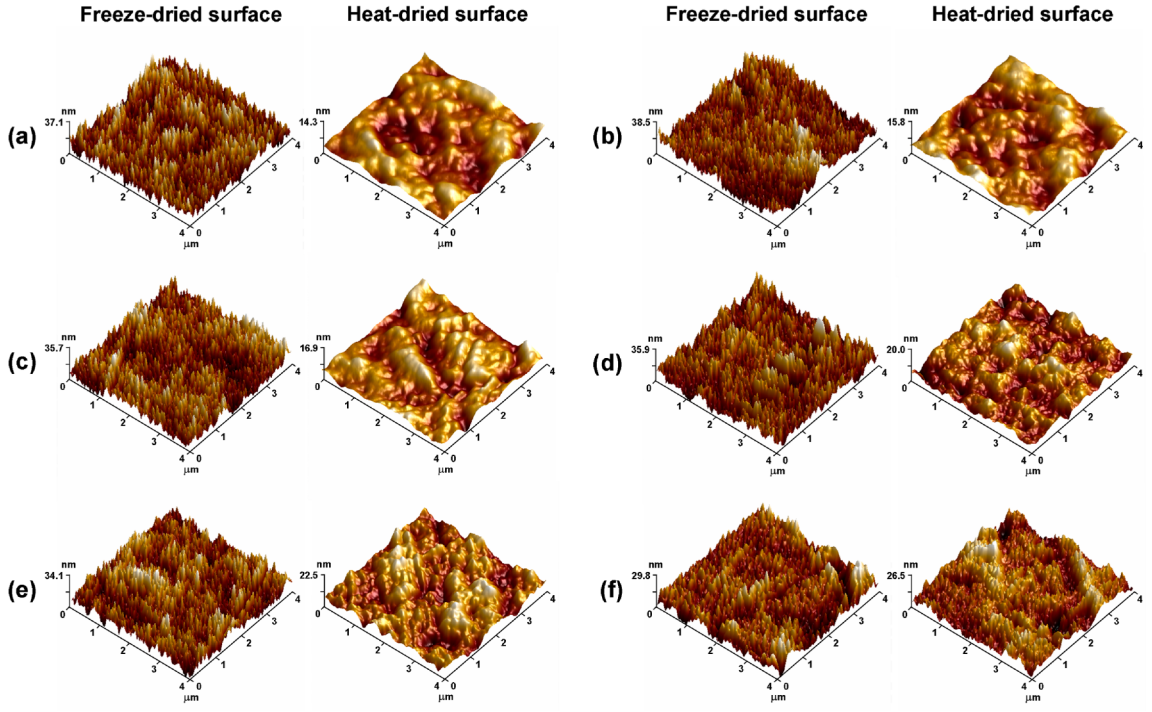

Figure 4. AFM topography images on polymer brush surfaces pretreated by the freeze-drying and heat-drying method, respectively: (a) PNIPAAm, (b) P(NIPAAm-2PEGMA), (c) P(NIPAAm-5PEGMA), (d) P(NIPAAm-9PEGMA), (e) P(NIPAAm-13PEGMA), and (f) P(PEGMA).

calculated and their values are listed in Table 1. The freeze-dried surfaces gave larger roughness values than the heat-dried surfaces, confirming the stretching−shrinking change of the thermosensitive brushes. It is evident that the stretched chain can induce larger roughness on the surface and the shrunk chain can induce smaller roughness on the surface. With increase of the PEGMA content, however, the thermosensitive brushes presented increased roughness on the heat-dried surface, when their roughness values remained approximately constant on the freeze-dried surface. These roughness changes diminished the roughness ratio and reveal that the hydrophilic PEGMA comonomer inclines to weaken the stretching−shrinking transition of the copolymer brushes. The larger roughness ratios of P(NIPAAm-2PEGMA) and P(NIPAAm-5PEGMA), which were close to that of PNIPAAm, indicate their reservation of the stronger chain stretching−shrinking change in the volume-phase transition.

Table 1. RMS Roughness of Polymer Brush Surfaces Obtained from AFM Results of Figure 4

	RMS roughness (nm)		
polymer brush	freeze-dried surface	heat-dried surface	roughness ratio
PNIPAAm	7.81	3.02	2.59
P(NIPAAm-2PEGMA)	7.59	3.13	2.42
P(NIPAAm-5PEGMA)	7.66	3.75	2.04
P(NIPAAm-9PEGMA)	7.59	4.41	1.72
P(NIPAAm-13PEGMA)	7.53	5.03	1.50
P(PEGMA)	6.11	5.61	1.09

3.5. Surface Self-Cleaning. According to the washing principle described by Kling,[45,47] an oil droplet is self-detachable from a hydrophilic surface if its underwater contact angle reaches 180°. However, it is seldom that an oil pollutant can exhibit such underwater superoleophobicity even on a surface with good hydrophilicity. Hence an external mechanical force is usually required for assisting the oil detachment from the surface, as indicated by the residual work theory of eq 4. Following these washing principles, the P(NIPAAm-PEGMA) copolymer brushes have great potentials to present the self-cleaning performance based on their good surface hydrophilicity and inherent washing force provided by the intense conformation transition of chain stretching and shrinking.

As mentioned above, all thermosensitive brushes could finish their volume-phase transitions at temperatures of 25 and 50 °C (see Figure 2a and Supporting Information Figure S3). In consideration of comparable convenience among the series of thermosensitive brushes, both fixed temperatures of 25 and 50 °C were adopted in the self-cleaning evaluation. After immersing the fouled sample into water at 25 and 50 °C, respectively, oil residues on the surface were weighed for quantitative evaluation of its self-cleaning capability. As seen in the oil residue results of Figure 5a, both PNIPAAm and P(NIPAAm-2PEGMA) surfaces left larger quantities of oil residues due to their surface hydrophobicity above the LCSTs. Similarly, lots of oil pollutants were reserved on the hydrophilic surface of P(PEGMA), proving that the oil pollutant is not self-detachable from the hydrophilic surface with the water contact angle of 40° or oil contact angle of 163° (see Figure 2a,b). The thorough oil removal from the P(PEGMA) surface, which occurred in the adhesive force measurement of Figure 3b, is ascribed to the external force endowed upon the oil droplet by the metal O-ring. This external force could provide the residual work to drive the oil contact angle to 180°. Once the PEGMA content exceeded 5 mol % for the P(NIPAAm-PEGMA) surfaces (Figure 5a), however, the oil residues were greatly reduced relative to other surfaces. After three cleaning cycles, there were only 0.2, 1.1, and 1.6 wt % of oil residues left on surfaces of P(NIPAAm-5PEGMA), P(NIPAAm-9PEGMA),

DOI: 10.1021/acsami.5b07336
ACS Appl. Mater. Interfaces 2015, 7, 22128−22136

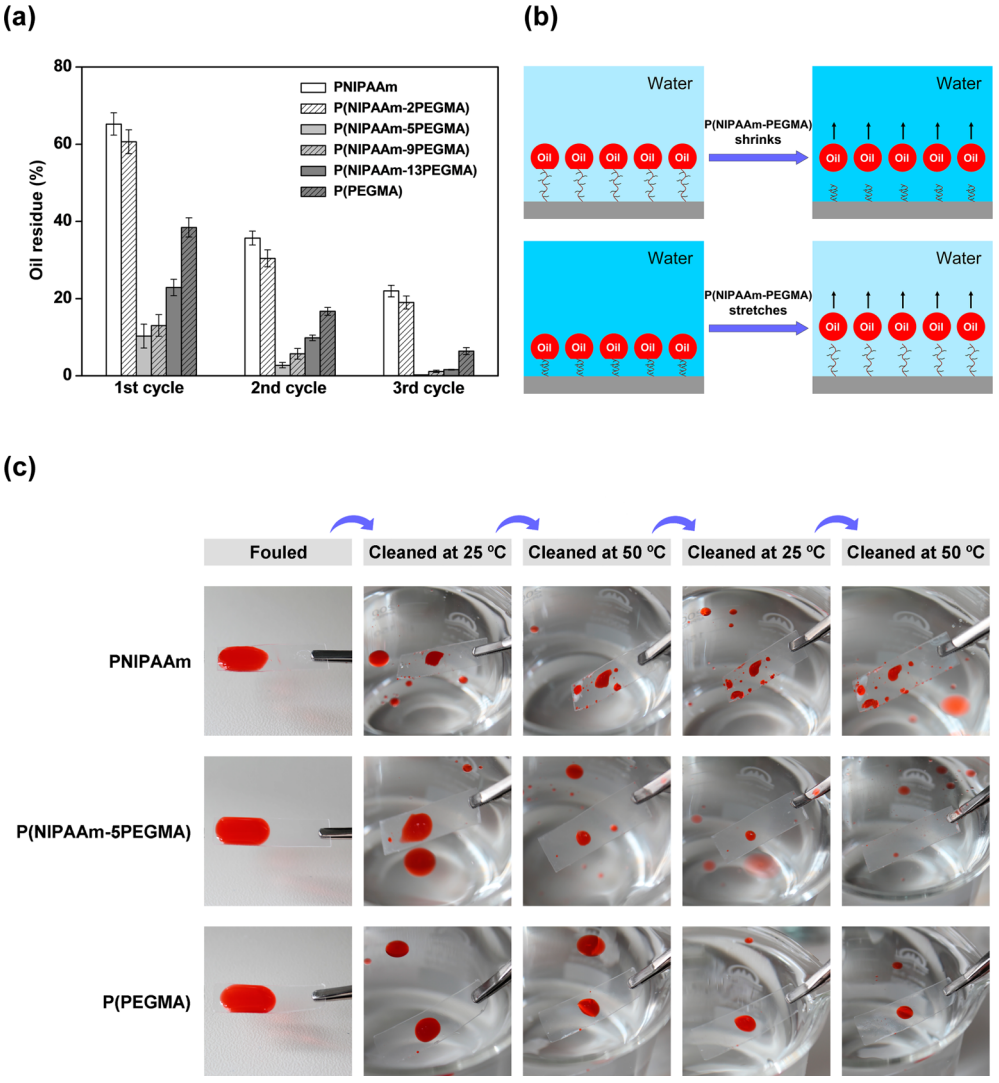

Figure 5. (a) Oil residues on polymer brush surfaces after three temperature-change water cleaning cycles performed at 25 and 50 °C, respectively. (b) Schematic illustration of temperature-change water cleaning of the thermosensitive P(NIPAAm-PEGMA) brush surface. (c) Images of polymer brush surfaces fouled by oil (red) and cleaned after the temperature-change water cleaning cycles.

and P(NIPAAm-13PEGMA), respectively. This efficient cleaning is evidently ascribed to their both surface characters of good hydrophilicity and the conformation transition of chain stretching and shrinking in the volume-phase transition. The hydrophilic surface can facilitate oil detachment via reducing oil adhesion, and simultaneously the conformation transition can provide the inherent washing force to promote oil detachment, as sketched in Figure 5b. Among the three copolymers, however, P(NIPAAm-5PEGMA) reached the optimal surface cleaning. Although P(NIPAAm-5PEGMA) achieved a water contact angle of 66° above the LCST, which was slightly higher than those of P(NIPAAm-9PEGMA) and P(NIPAAm-13PEGMA), its conformation transition was more sensitive and intense, as proved in the AFM results. These balanced surface features in hydrophilicity and the sharp volume-phase transition, which are absent for other P(NIPAAm-PEGMA) copolymers, endow the P(NIPAAm-5PEGMA) surface with the excellent self-cleaning performance. In view of the relatively stable surface wettability at temperatures outside the range of the volume-phase transition (Figure 2a) and thermal insensibility of oil property and water property, it can be speculated that the thermosensitive brushes exhibit the similar self-cleaning performances if the measurement temperature is set at that slightly below 25 °C or above 50 °C. In addition to the model oil of hexadecane used in this work, the self-cleaning surface thus demonstrated could be potentially applicable for cleaning many other organic contaminants, such as protein, humic acid, and mineral oil, in the field of membrane separation or oil/water separation.

The cleaning performances of the modified surfaces are visible from their images in processes of the temperature-change cleaning, as shown in Figure 5c. The oil was dyed red for easy distinguishing in the images. After both cleaning cycles were performed at 25 and 50 °C, respectively, the hydrophilic surface of P(PEGMA) showed the limited cleaning ability with considerable amounts of oil residues reserved on the surface, proving that the hydrophilic surface cannot solely achieve the thorough removal of oil pollutants. The PNIPAAm brush would rather adsorb oil pollutes on its hydrophobic surface at 50 °C than on its hydrophilic surface at 25 °C (after each washing, water was refreshed). This washing result of PNIPAAm confirms its great defect of surface hydrophobicity in removing oil pollutants, even if a sharp conformation transition can be provided in its volume-phase transition. As

DOI: 10.1021/acsami.5b07336
ACS Appl. Mater. Interfaces 2015, 7, 22128−22136

expected, the best cleaning performance was reached by the P(NIPAAm-5PEGMA) surface, when fewer oil residues were left after both cleaning cycles. This excellent cleaning performance is absent for homopolymer brushes of PNIPAAm and P(PEGMA). Hence both surface hydrophilicity and the sharp conformation transition of chain stretching and shrinking are necessary factors for the thermosensitive polymers to achieve surface self-cleaning.

4. CONCLUSIONS

Thermoresponsive copolymer brushes of P(NIPAAm-PEGMA) were fabricated on the PP surface for constructing the underwater self-cleaning surface. Hydrophilic surfaces with water contact angles below 66° were obtained from the copolymer brushes with the PEGMA content exceeding 5 mol %, whenever at temperatures below or above their LCSTs. Hence their underwater oleophobicity was greatly improved, when higher contact angles, lower adhesion works, lower residual works, and lower adhesive forces of oil pollutants were reached. In addition, the sharp volume-phase transition feature was reserved in the copolymer backbones, as proved by the AFM result. Self-cleaning evaluation on the modified surfaces was carried out by a simple temperature-change water cleaning method, after which only 0.2, 1.1, and 1.6 wt % of oil residues remained on surfaces of P(NIPAAm-5PEGMA), P(NIPAAm-9PEGMA), and P(NIPAAm-13PEGMA), respectively. These good surface self-cleaning capabilities were absent for homopolymer brushes of PNIPAAm and P(PEGMA). It is reasonable to conclude that both hydrophilicity and the conformation change of chain stretching and shrinking are two crucial factors for the surfaces to present the underwater self-cleaning performances. This study contributes to development of the underwater self-cleaning surface based on a hydrophilic surface with the chain motion.

■ ASSOCIATED CONTENT

Supporting Information

The Supporting Information is available free of charge on the ACS Publications website at DOI: 10.1021/acsami.5b07336.

Schematic illustration of oil detachment from an underwater solid surface with the help of the washing force; peak area ratios for P(NIPAAm-PEGMA) brushes obtained from FT-IR results of Figure 1a; transmittance of thermosensitive polymers as a function of the temperature; force changes in adhesive force measurements when oil droplets were being drawn away from polymer brush surfaces (PDF)

■ AUTHOR INFORMATION

Corresponding Author

*E-mail: jhuang@njtech.edu.cn.

Notes

The authors declare no competing financial interest.

■ ACKNOWLEDGMENTS

This work was supported by the National Basic Research Program of China (Grant 2009CB623404), the National Natural Science Foundation of China (Grant 20476045), and the Priority Academic Program Development of Jiangsu Higher Education Institutions (PAPD).

■ REFERENCES

(1) Liu, K.; Jiang, L. Bio-Inspired Self-Cleaning Surfaces. *Annu. Rev. Mater. Res.* **2012**, *42*, 231−263.
(2) Leng, B.; Shao, Z.; de With, G.; Ming, W. Superoleophobic Cotton Textiles. *Langmuir* **2009**, *25*, 2456−2460.
(3) Zhao, H.; Law, K. Y. Directional Self-Cleaning Superoleophobic Surface. *Langmuir* **2012**, *28*, 11812−11818.
(4) Jiang, W.; Grozea, C. M.; Shi, Z.; Liu, G. Fluorinated Raspberry-Like Polymer Particles for Superamphiphobic Coatings. *ACS Appl. Mater. Interfaces* **2014**, *6*, 2629−2638.
(5) Jin, M.; Wang, J.; Yao, X.; Liao, M.; Zhao, Y.; Jiang, L. Underwater Oil Capture by a Three-Dimensional Network Architectured Organosilane Surface. *Adv. Mater.* **2011**, *23*, 2861−2864.
(6) Jung, Y. C.; Bhushan, B. Wetting Behavior of Water and Oil Droplets in Three-Phase Interfaces for Hydrophobicity/philicity and Oleophobicity/philicity. *Langmuir* **2009**, *25*, 14165−14173.
(7) Liu, M.; Wang, S.; Wei, Z.; Song, Y.; Jiang, L. Bioinspired Design of a Superoleophobic and Low Adhesive Water/Solid Interface. *Adv. Mater.* **2009**, *21*, 665−669.
(8) Liu, Q.; Patel, A. A.; Liu, L. Superhydrophilic and Underwater Superoleophobic Poly(sulfobetaine methacrylate)-Grafted Glass Fiber Filters for Oil-Water Separation. *ACS Appl. Mater. Interfaces* **2014**, *6*, 8996−9003.
(9) Zhang, W.; Zhu, Y.; Liu, X.; Wang, D.; Li, J.; Jiang, L.; Jin, J. Salt-Induced Fabrication of Superhydrophilic and Underwater Superoleophobic PAA-g-PVDF Membranes for Effective Separation of Oil-in-Water Emulsions. *Angew. Chem., Int. Ed.* **2014**, *53*, 856−860.
(10) Lin, L.; Liu, M.; Chen, L.; Chen, P.; Ma, J.; Han, D.; Jiang, L. Bio-Inspired Hierarchical Macromolecule−Nanoclay Hydrogels for Robust Underwater Superoleophobicity. *Adv. Mater.* **2010**, *22*, 4826−4830.
(11) Cao, Y.; Liu, N.; Fu, C.; Li, K.; Tao, L.; Feng, L.; Wei, Y. Thermo and pH Dual-Responsive Materials for Controllable Oil/Water Separation. *ACS Appl. Mater. Interfaces* **2014**, *6*, 2026−2030.
(12) Liu, X.; Gao, J.; Xue, Z.; Chen, L.; Lin, L.; Jiang, L.; Wang, S. Bioinspired Oil Strider Floating at the Oil/Water Interface Supported by Huge Superoleophobic Force. *ACS Nano* **2012**, *6*, 5614−5620.
(13) Gondal, M. A.; Sadullah, M. S.; Dastageer, M. A.; McKinley, G. H.; Panchanathan, D.; Varanasi, K. K. Study of Factors Governing Oil-Water Separation Process Using TiO_2 Films Prepared by Spray Deposition of Nanoparticle Dispersions. *ACS Appl. Mater. Interfaces* **2014**, *6*, 13422−13429.
(14) Arndt, M. C.; Sadowski, G. Modeling Poly(N-isopropylacrylamide) Hydrogels in Water/Alcohol Mixtures with PC-SAFT. *Macromolecules* **2012**, *45*, 6686−6696.
(15) Adam, N. K.; Stevenson, D. G. Detergent Action. *Endeavour* **1953**, *12*, 25−32.
(16) Kao, R. L.; Wasan, D. T.; Nikolov, A. D.; Edwards, D. A. Mechanisms of Oil Removal from a Solid Surface in the Presence of Anionic Micellar Solutions. *Colloids Surf.* **1988**, *34*, 389−398.
(17) Thompson, L. The Role of Oil Detachment Mechanisms in Determining Optimum Detergency Conditions. *J. Colloid Interface Sci.* **1994**, *163*, 61−73.
(18) Kissa, E. Kinetics and Mechanisms of Detergency Part I: Liquid Hydrophobic (Oily) Soils. *Text. Res. J.* **1975**, *45*, 736−741.
(19) Lee, A.; Seo, M. H.; Yang, S.; Koh, J.; Kim, H. The Effects of Mechanical Actions on Washing Efficiency. *Fibers Polym.* **2008**, *9*, 101−106.
(20) Heskins, M.; Guillet, J. E. Solution Properties of Poly(N-isopropylacrylamide). *J. Macromol. Sci., Chem.* **1968**, *2*, 1441−1455.
(21) Lele, A. K.; Devotta, I.; Mashelkar, R. A. Predictions of Thermoreversible Volume Phase Transitions in Copolymer Gels by Lattice-Fluid-Hydrogen-Bond Theory. *J. Chem. Phys.* **1997**, *106*, 4768−4772.
(22) Brazel, C. S.; Peppas, N. A. Synthesis and Characterization of Thermo- and Chemomechanically Responsive Poly(N-isopropylacrylamide-co-methacrylic acid) Hydrogels. *Macromolecules* **1995**, *28*, 8016−8020.

DOI: 10.1021/acsami.5b07336
ACS Appl. Mater. Interfaces 2015, 7, 22128−22136

(23) Abu-Lail, N. I.; Kaholek, M.; LaMattina, B.; Clark, R. L.; Zauscher, S. Micro-Cantilevers with End-Grafted Stimulus-Responsive Polymer Brushes for Actuation and Sensing. *Sens. Actuators, B* **2006**, *114*, 371−378.
(24) Guo, H.; Huang, J.; Wang, X. The Alternate Temperature-Change Cleaning Behaviors of PNIPAAm Grafted Porous Polyethylene Membrane Fouled by Proteins. *Desalination* **2008**, *234*, 42−50.
(25) Zhou, S.; Xue, A.; Zhang, Y.; Li, M.; Wang, J.; Zhao, Y.; Xing, W. Fabrication of Temperature-Responsive ZrO_2 Tubular Membranes, Grafted with Poly(N-isopropylacrylamide) Brush Chains, for Protein Removal and Easy Cleaning. *J. Membr. Sci.* **2014**, *450*, 351−361.
(26) Yu, S.; Chen, Z.; Liu, J.; Yao, G.; Liu, M.; Gao, C. Intensified Cleaning of Organic-Fouled Reverse Osmosis Membranes by Thermo-Responsive Polymer (TRP). *J. Membr. Sci.* **2012**, *392*−*393*, 181−191.
(27) Chen, W.; Qu, L.; Chang, D.; Dai, L.; Ganguli, S.; Roy, A. Vertically-Aligned Carbon Nanotubes Infiltrated with Temperature-Responsive Polymers: Smart Nanocomposite Films for Self-Cleaning and Controlled Release. *Chem. Commun.* **2008**, 163−165.
(28) Cho, E. C.; Kim, Y. D.; Cho, K. Temperature-Dependent Intermolecular Force Measurement of Poly(N-isopropylacrylamide) Grafted Surface with Protein. *J. Colloid Interface Sci.* **2005**, *286*, 479−486.
(29) Burkert, S.; Bittrich, E.; Kuntzsch, M.; Müller, M.; Eichhorn, K. J.; Bellmann, C.; Uhlmann, P.; Stamm, M. Protein Resistance of PNIPAAm Brushes: Application to Switchable Protein Adsorption. *Langmuir* **2010**, *26*, 1786−1795.
(30) Perry, S. S.; Yan, X.; Limpoco, F. T.; Lee, S.; Müller, M.; Spencer, N. D. Tribological Properties of Poly(L-lysine)-graft-poly(ethylene glycol) Films: Influence of Polymer Architecture and Adsorbed Conformation. *ACS Appl. Mater. Interfaces* **2009**, *1*, 1224−1230.
(31) Cappelli, A.; Galeazzi, S.; Giuliani, G.; Anzini, M.; Grassi, M.; Lapasin, R.; Grassi, G.; Farra, R.; Dapas, B.; Aggravi, M.; Donati, A.; Zetta, L.; Boccia, A. C.; Bertini, F.; Samperi, F.; Vomero, S. Synthesis and Spontaneous Polymerization of Oligo(ethylene glycol)-Conjugated Benzofulvene Macromonomers. A Polymer Brush Forming a Physical Hydrogel. *Macromolecules* **2009**, *42*, 2368−2378.
(32) Yu, Y.; Chen, C. K.; Law, W. C.; Sun, H.; Prasad, P. N.; Cheng, C. A Degradable Brush Polymer−Drug Conjugate for pH-Responsive Release of Doxorubicin. *Polym. Chem.* **2015**, *6*, 953−961.
(33) Winblade, N. D.; Schmökel, H.; Baumann, M.; Hoffman, A. S.; Hubbell, J. A. Sterically Blocking Adhesion of Cells to Biological Surfaces with a Surface-Active Copolymer Containing Poly(ethylene glycol) and Phenylboronic Acid. *J. Biomed. Mater. Res.* **2002**, *59*, 618−631.
(34) Bayramoglu, G.; Akcalı, K. C.; Gultekin, S.; Bengu, E.; Arica, M. Y. Preparation and Characterization of Poly(hydroxyethyl methacrylate-co-poly(ethyleneglycol-methacrylate)/Hydroxypropyl-chitosan) Hydrogel Films: Adhesion of Rat Mesenchymal Stem Cells. *Macromol. Res.* **2011**, *19*, 385−395.
(35) Ma, X.; Xi, J.; Zhao, X.; Tang, X. Deswelling Comparison of Temperature-Sensitive Poly(N-isopropylacrylamide) Microgels Containing Functional-OH Groups with Different Hydrophilic Long Side Chains. *J. Polym. Sci., Part B: Polym. Phys.* **2005**, *43*, 3575−3583.
(36) Ma, X.; Huang, X.; Zhu, L.; Zhao, X.; Tang, X. Influence of Ethyl Methacrylate Content on the Volume-Phase Transition of Temperature-Sensitive Poly[(N-isopropylacrylamide)-co-(ethyl methacrylate)] Microgels. *Polym. Int.* **2005**, *54*, 83−89.
(37) Kwon, O. H.; Kikuchi, A.; Yamato, M.; Okano, T. Accelerated Cell Sheet Recovery by Co-Grafting of PEG with PIPAAm onto Porous Cell Culture Membranes. *Biomaterials* **2003**, *24*, 1223−1232.
(38) Tomer, N.; Mondal, S.; Wandera, D.; Wickramasinghe, S. R.; Husson, S. M. Modification of Nanofiltration Membranes by Surface-Initiated Atom Transfer Radical Polymerization for Produced Water Filtration. *Sep. Sci. Technol.* **2009**, *44*, 3346−3368.
(39) Wandera, D.; Wickramasinghe, S. R.; Husson, S. M. Modification and Characterization of Ultrafiltration Membranes for Treatment of Produced Water. *J. Membr. Sci.* **2011**, *373*, 178−188.
(40) Wandera, D.; Himstedt, H. H.; Marroquin, M.; Wickramasinghe, S. R.; Husson, S. M. Modification of Ultrafiltration Membranes with Block Copolymer Nanolayers for Produced Water Treatment: The Roles of Polymer Chain Density and Polymerization Time on Performance. *J. Membr. Sci.* **2012**, *403*−*404*, 250−260.
(41) Shi, S.; Zhou, Y.; Lu, X.; Ye, Y.; Huang, J.; Wang, X. Plasma-Initiated DT Graft Polymerization of Acrylic Acid on Surface of Porous Polypropylene Membrane for Pore Size Control. *Plasma Chem. Plasma Process.* **2014**, *34*, 1257−1269.
(42) Ma, J.; Luan, S.; Song, L.; Jin, J.; Yuan, S.; Yan, S.; Yang, H.; Shi, H.; Yin, J. Fabricating a Cycloolefin Polymer Immunoassay Platform with a Dual-Function Polymer Brush via a Surface-Initiated Photoiniferter-Mediated Polymerization Strategy. *ACS Appl. Mater. Interfaces* **2014**, *6*, 1971−1978.
(43) Wu, D.; Liu, X.; Yu, S.; Liu, M.; Gao, C. Modification of Aromatic Polyamide Thin-Film Composite Reverse Osmosis Membranes by Surface Coating of Thermo-Responsive Copolymers P(NIPAM-co-Am). I: Preparation and Characterization. *J. Membr. Sci.* **2010**, *352*, 76−85.
(44) Clint, J. H.; Wicks, A. C. Adhesion under Water: Surface Energy Considerations. *Int. J. Adhes. Adhes.* **2001**, *21*, 267−273.
(45) Kling, W.; Lange, H. Zur Energetik des Waschvorganges bei ö1igen Anschmutzungen. *Colloid Polym. Sci.* **1955**, *142*, 1−5.
(46) Alexandrov, A. D.; Toshev, B. V.; Scheludko, A. D. Nucleation from Supersaturated Water Vapors on n-Hexadecane: Temperature Dependence of Critical Supersaturation and Line Tension. *Langmuir* **1991**, *7*, 3211−3215.
(47) Kling, W. Der Waschvorgang als Umnetzung. *Colloid Polym. Sci.* **1949**, *115*, 37−44.

DOI: 10.1021/acsami.5b07336
ACS Appl. Mater. Interfaces 2015, 7, 22128−22136